Practical Solid-Phase Parallel Synthesis of Δ^5-2-Oxopiperazines via *N*-Acyliminium Ion Cyclization

Sung-Chan Lee and Seung Bum Park*

Department of Chemistry, Seoul National University, Seoul 151-747, Korea

Received March 20, 2007

A practical solid-phase strategy for the synthesis of Δ^5-2-oxopiperazines via *N*-acyliminium ion cyclization has been developed. A key step in the library synthesis is tandem acidolytic cleavage with subsequent in situ iminium formation, followed by stable enamide transformation. This approach is exemplified by the preparation of a 192-member pilot library using bromoacetal resins without further purification.

Introduction

It is well-known that piperazines, diketopiperazines, and piperazinones are important pharmacophores that are used as peptidomimetic moieties for the discovery of novel bioactive small molecules.[1] The transformation of peptides into conformationally restricted peptide analogs is a generally accepted approach to design nonpeptide ligands that target protein receptors. Peptidyl-prolyl isomerase inhibitor,[2a] chymase inhibitor,[2b] substance P antagonist,[3] bradykinin receptor antagonist,[4] and geranylgeranyl transferase I (GGTase-I) and farnesyl transferase (FTase) inhibitors[5] are excellent examples of peptidomimetic drugs discovered using oxopiperazine as a simple, yet critical, core skeleton that conformationally mimics the dipeptide moiety. Some of these targets are typical G-protein-coupled receptors with seven putative membrane-spanning regions, which are used for the perturbation of their functions with peptidomimetic ligands.[6−8] FTase and GGTase-I are also promising molecular targets, and the small molecule peptoid inhibitors as substrate mimics of these enzymes can specifically block the malignant transformation caused by mutated Ras proteins. In particular, GGTase-I has attracted attention because of its critical role in the promotion of tumorigenesis and metastasis through a complex signaling pathway with various substrates such as RhoC, RhoA, Rac-1, Cdc42, R-Ras, and TC-21.[5,9]

In terms of chemistry, several synthetic methods for obtaining piperazinones, which are generally reduced from Δ^5-2-oxopiperazines, in the solution phase have been reported.[10,14,15] We are particularly interested in the Δ^5-2-oxopiperazine core skeleton, which is a highly conserved and unsaturated cyclic structure, as a remarkable pharmacophore. As shown in Figure 1, 5,6-unsaturated oxopiperazines mimic dipeptide motifs and are incorporated in many drug candidates. However, there are few examples of synthetic exercises aimed at obtaining Δ^5-2-oxopiperazines in the solid phase. Cheng et al. have developed an interesting methodology for the synthesis of Δ^5-2-oxopiperazines in the solid phase by the Ugi multicomponent reaction.[13] However,

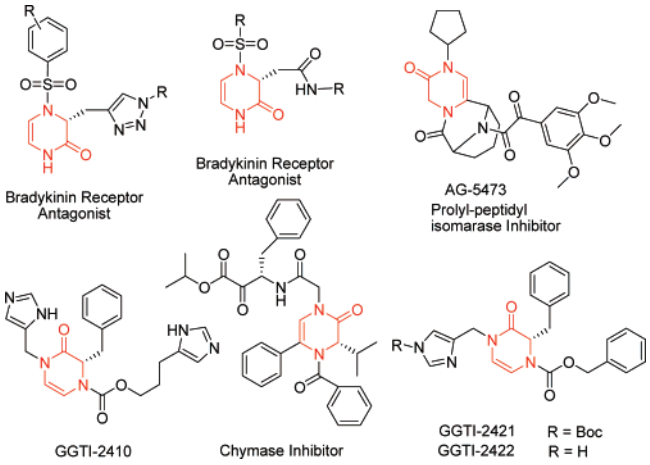

Figure 1. Bioactive Δ^5-2-oxopiperazines currently under the drug development.

this methodology has some limitations; in particular, it is not applicable to the practical construction of a diverse library. In our approach, we aimed for the development of a practical procedure for efficient synthesis of a privileged Δ^5-2-oxopiperazine core skeleton with imbedded diversification potentials through solid-phase parallel synthesis; this approach requires validation by the successful construction of a pilot library.

Many of the platforms employed in the discovery of new biologically active compounds have impacted the pharmaceutical industry. One such platform that has made the most significant impact is the systematic high-throughput screening of small molecule collections, termed libraries, created by combinatorial chemistry. Therefore, the combinatorial synthesis of large arrays of diverse compounds is now an important component of the modern drug discovery process in the early lead generation stage. Because of the high compatibility of high-throughput screening, a combinatorial library should be constructed by consideration of its practical application in various screening platforms. In particular, a combination of various techniques is required to address current bottlenecks in drug discovery, involving biological target validation of small molecule modulators, which deserve special emphasis. One technology platform that

* To whom correspondence should be addressed. E-mail: sbpark@snu.ac.kr.

10.1021/cc0700492 CCC: $37.00
Published on Web 06/26/2007

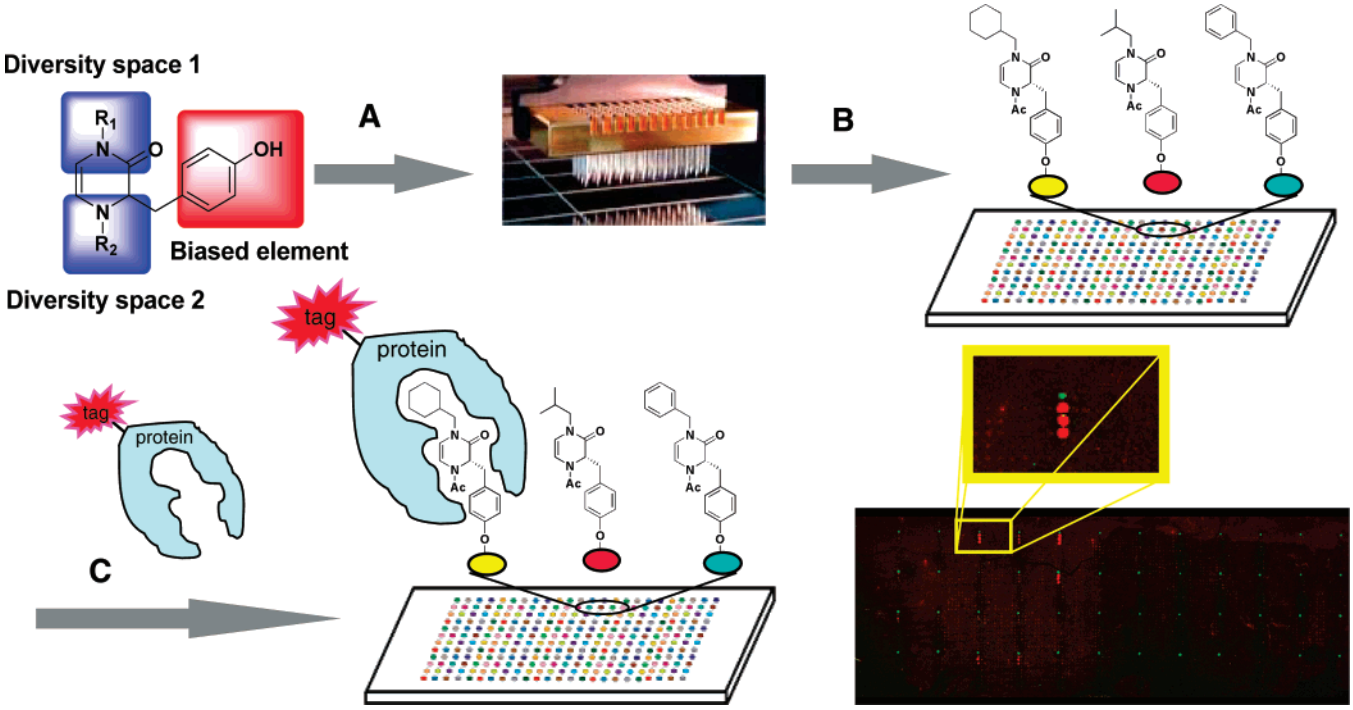

Figure 2. Strategy of a pilot library for the application in a small molecule microarray: (A) preparation of small molecule libraries with a common functional handle; (B) creation of small molecule microarrays on a chemically modified glass chip; (C) incubation of fluorescently labeled proteins of interest, followed by detection with a standard fluorescent slide scanner.

addresses this issue is a combination of cell-based high-throughput screening with proteomic screening using a small molecule microarray. Small molecule microarrays have been proven to be a discovery tool for the identification of novel putative interactions between proteins and small molecules; these interactions are typically visualized by using fluorescently labeled proteins or antibodies with a standard fluorescence slide scanner.[16−19] The principle of small molecule microarrays is the same as that of DNA or protein microarrays; while a DNA or protein microarray immobilizes nucleotides or proteins on a glass chip, a small molecule microarray immobilizes an array of small molecules with covalent linkages through functional-group-specific chemical reactions.[19] Therefore, it is important to create a library with common functional handles for application in small molecule microarray technology. In addition, a common functional group can provide an attachment point for affinity chromatography in target identification and drug delivery systems. Therefore, we introduced a phenolic hydroxyl group into our core skeleton not only as a common functional handle for efficient immobilization on a glass surface but also as a potential partner for interaction with biopolymers (see Figure 2).

The *N*-acyliminium-type nucleophilic tandem cyclization has been recognized as a powerful reaction for the construction of heterocyclic and bicyclic ring systems in solid- and solution-phase syntheses.[11,12,20] The key intermediates in this reaction, namely, *N*-acyliminium ions, are excellent electrophiles that react with many different types of nucleophiles such as oxygen, nitrogen, sulfur, and even electron-rich aromatic carbon. In our previous study, we successfully demonstrated a practical application of the Pictet−Spengler intramolecular cyclization of *N*-acyliminium ions with carbon nucleophiles (Path A in Figure 3).[22] In this study, we have developed a unique reaction pathway to generate stable Δ^5-2-oxopiperazines from intracyclic *N*-acyliminum ions by acid-catalyzed rearrangement without intra- or intermolecular nucleophilic substitution (Path B in Figure 3).

Results and Discussion

The key aspects of this transformation are the electronic effect of R_3 substituents on in situ-generated unstable *N*-acyliminium and the development of an appropriate acidic condition for the generation of the Δ^5-2-oxopiperazine moiety.[21] The efficient rearrangement of *N*-acyliminium into enamide is influenced by the introduction of electron-withdrawing *N*-substituents (R_3 in Figure 3) such as carbonyl or amide. In addition to the effects of the substituents, the generation of the enamide moiety depends on the proton source for cyclization. Several acidic conditions for catalytic enamide cyclization have been developed using *p*-toluenesulfonic acid, TFA, HCl, H_2SO_4, etc.[10,14] However, the practical application of these previously reported reaction conditions for library construction is significantly limited by a tedious purification process and potential complications caused by residual acids in the assay system. It is also reported that a strong acid, high temperature, or both can facilitate the rearrangement of unsaturated oxopiperazine into the acyliminium intermediate, thereby reversing the desired transformation.[21] After extensively screening the reaction conditions, we have optimized the acid-catalyzed enamide cyclization by using neat formic acid, which is a relatively weak acid and can be easily removed by lyophilization.

The synthetic procedure for production of the unsaturated Δ^5-2-oxopiperazine moiety was developed through the optimization process using representative compounds with various R_3 substituents such as acetyl, benzyloxy carbonyl, and benzyl amido groups for the preparation of amide (**4a**),

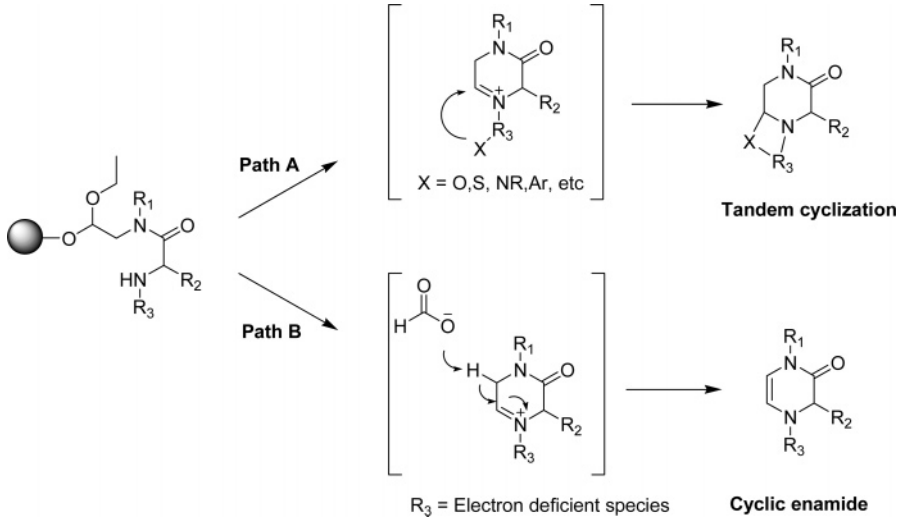

Figure 3. Two general pathways through the key acyliminium intermediate.

Scheme 1. Feasibility Test of Unsaturated Oxopiperazine Scaffold[a]

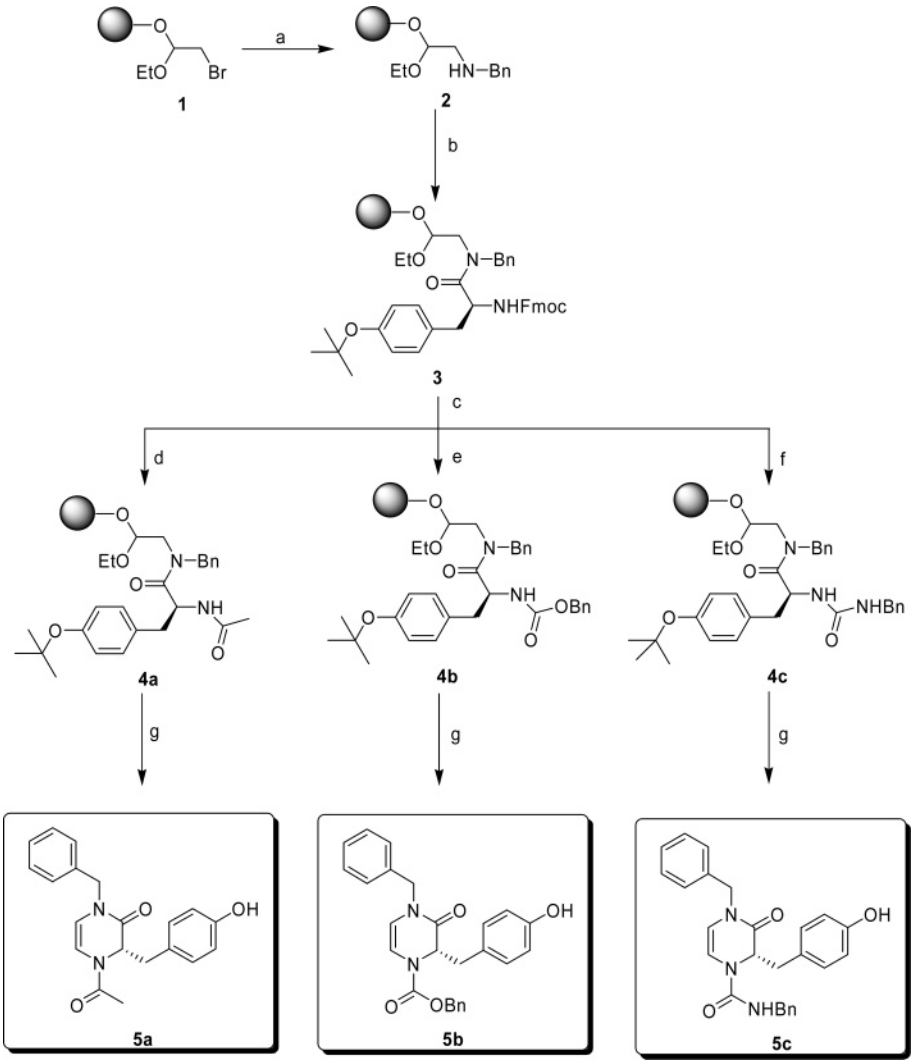

[a] Reagents and conditions: (a) $BnNH_2$, DMSO, 60 °C; (b) Fmoc(*O*-*t*-Bu)TyrOH, HATU, DIPEA, DMF, room temperature (RT); (c) 25% piperidine, RT; (d) Ac_2O, Py, DCE, RT; (e)BnOCOCl, DIPEA, DCE; (f) BnNCO, DIPEA, DCE, RT; (g) neat HCO_2H, 60 °C, 3 h.

carbamate (**4b**), and urea (**4c**), respectively. Other substituents, namely, R_1 and R_2, were fixed with benzyl and hydroxyl benzyl groups for easy comparison. As shown in Scheme 1, the representative compounds **5a**, **5b**, and **5c** were successfully synthesized in high yields and exceptional purities (>90%) using the optimized reaction condition on a solid support. However, significant amounts of byproducts were produced during the synthesis of the desired enamides even under the optimized reaction conditions in the case of electrically neutral proton or electron donating alkyl groups,

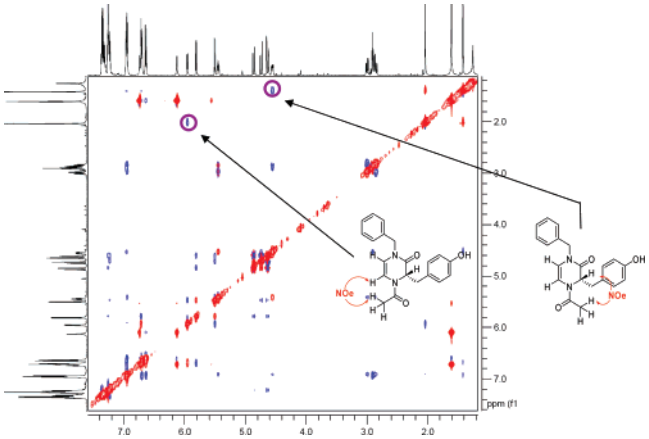

Figure 4. NOE correlation between two rotamers of the representative compound **5a**.

which were introduced by the reductive amination of aldehydes, at the R_3 position (data not shown). Therefore, we concluded that the in situ-generated *N*-acyliminium ion should be activated with an electron-withdrawing group for efficient rearrangement initiated by deprotonation for the synthesis of cyclic enamides (unsaturated Δ^5-2-oxopiperazines). Interestingly, **5a** and **5b** were identified as mixtures of two isomers by NMR analysis; however, they were inseparable in the reverse HPLC condition. By performing extensive NMR analysis, we could confirm that the two isomers were rotational isomers because of the rigid structure of the unsaturated oxopiperazine. As shown in Figure 4, the rotamers of **5a** were evidently obtained by the nuclear Overhauser effect (NOE) between acetyl and vinyl protons along with a tyrosine alpha proton (see Supporting Information).

After the confirmation of the selective and efficient monocyclization to unsaturated oxopiperazine in the solid phase, the pilot library with this core skeleton was designed using bromoacetal resin with the expectation of the tandem rearrangement in the cleavage step under a mild acidic condition. The library synthesis was initiated by the incorporation of the R_1 diversity element through the simple amination of primary amines on the bromoacetal resin (**1**) in DMSO solution at 60 °C. The bromoacetal resins used in this study were prepared in our laboratory from Wang resin to achieve high loading levels (loading level = 1.6 mmol/g). The resin-bound secondary amine (**6**) was coupled with Fmoc *N*-protected and *O*-*t*-Bu-protected tyrosine as a biasing element on the R_2 diversity element. Efficient amidation was achieved by the activation of carboxylic acid with HATU [*O*-(7-azabenzotriazole-1-yl)-*N*,*N*,*N*′,*N*′-tetramethyluronium PF_6], and the completion of the amidation step was monitored by a negative chloranil test. The R_3 diversity element was extensively explored by the modification of the Fmoc-deprotected primary amine on the solid support with various counterparts such as acid, carbamic chloride, and isocyanate for the introduction of amide, carbamate, and urea moieties on our core skeleton; the completion of this reaction step was monitored by the Kaiser test. The final step was carried out using neat formic acid to synchronize the compound cleavage from the solid support and the in situ generation of cyclic *N*-acyliminium ions followed by the

Scheme 2. General Scheme of Solid-Phase Synthesis Strategy[a]

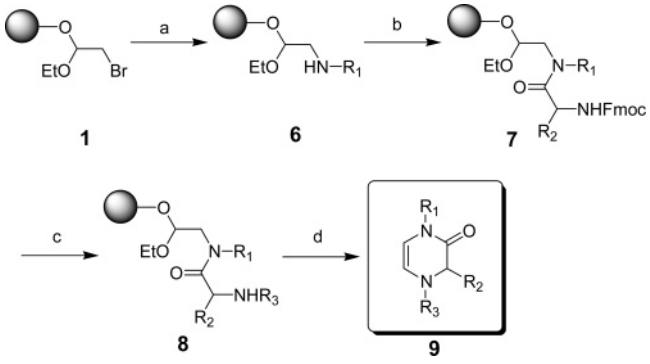

[a] Reagents and conditions: (a) R_1NH_2, DMSO, 60 °C; (b) Fmoc(*O*-*t*-Bu)TyrOH, HATU, DIPEA, DMF, RT; (c) (1) 25% piperidine, RT, (2) RCO_2H, DIC, HOBt, DIPEA, RT, (3) ROCOCl, DIPEA, DCE, RT, (4) RNCO, DIPEA, DCE, RT; (d) neat HCO_2H, 60 °C.

rearrangement to Δ^5-2-oxopiperazines: three key chemical transformations in a single step with high efficiency. The final cleavage/cyclization step successfully provided the desired monocycle product in high yields and purities without any nonvolatile side products, thereby ensuring high efficiency of the library construction (Scheme 2).

A practical solid-phase synthesis library with the Δ^5-2-oxopiperazine core skeleton was successfully constructed in a parallel 96-deep-well filtration block platform. The molecular diversity of the core skeleton was expanded by the introduction of various R_1 groups using commercially available primary amine, as shown in Table 1. At the R_2 position, significant diversification can be achieved simply by the amide coupling of various natural and unnatural amino acids. However, we weighted this pilot library with a single modification of tyrosine at the R_2 position, which introduces a phenolic functional handle for specific immobilization on the surface of a biochip and for affinity chromatography, an essential process for target identification. The apparent diversification at the R_2 position was validated by the successful introduction of different amino acids such as Phe and Asp by an identical procedure (data not shown), and further diversification of the R_2 position will be explored during focused library construction in due course. Finally, a series of commercially available carboxylic acids, chloroformates, and isocyanate were employed as R_3 diversity elements (see Table 1). To construct the pilot library by solid-phase parallel synthesis, 40 mg of high-loading bromoacetal resin (1.6 mmol/g) was used per library member: a process that yielded 10∼20 mg of final products without any further purification.

After the completion of the library construction, aliquots of the crude final products were concentrated using a 96-well platform evaporator and were diluted with acetonitrile. The purities and identities of all the library members were assessed by the direct analysis of the crude final products using LC/MS (Table 1). The presence of all the desired compounds was unambiguously confirmed by the molecular mass with an excellent purity range, as determined by the HPLC analysis using a PDA detector. The purity of each compound is shown in a different color in Table 1. Table 2 shows the crude analysis results of six representative library

Table 1. Structures and Purities of All Library Members

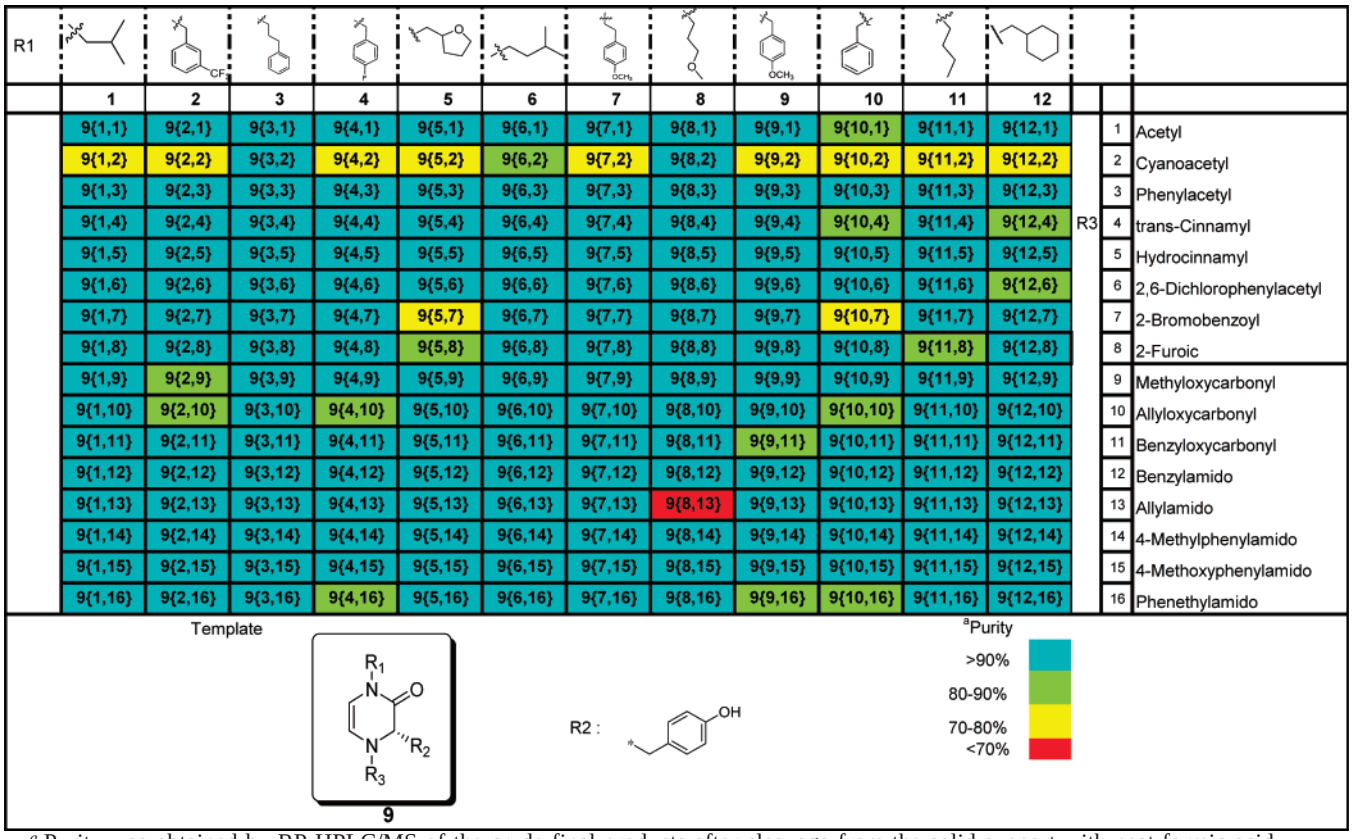

[a] Purity was obtained by RP-HPLC/MS of the crude final products after cleavage from the solid support with neat formic acid.

Table 2. Yield, Purity, and Mass of Each Representative Library Member

	R_1	R_2	R_3	yield[a] (%)	purity[b] (%)	MS (calcd)	MS (found)
9{*1, 3*}	isobutyl	4-hydroxybenzyl	phenylacetyl	83.3	92.9	379.20	379.15
9{*3, 3*}	3-phenylpropyl	4-hydroxybenzyl	phenylacetyl	71.4	91.9	441.21	441.16
9{*5, 9*}	tetrahydrofuranyl	4-hydroxybenzyl	methoxycarbonyl	90.9	92.7	347.16	346.99
9{*6, 9*}	isoamyl	4-hydroxybenzyl	methoxycarbonyl	95.2	94.5	333.18	333.04
9{*8, 12*}	3-methoxypropyl	4-hydroxybenzyl	phenethylamido	74.1	95.5	424.22	424.18
9{*12, 12*}	cyclohexylmethyl	4-hydroxybenzyl	phenethylamido	72.3	96.6	448.26	448.21

[a] Yields were calculated based on the loading level of initial bromoacetal resins. [b] Purities were obtained by RP-HPLC/MS of crude final products after cleavage from solid support.

members with their complete spectral data (see Experimental Section). In general, the average purity of the library is 90%, and the purities of more than 90% of the crude library members exceed 85%.

Conclusion

In conclusion, we successfully demonstrated the practical solid-phase synthesis of Δ^5-2-oxopiperazines. The key synthetic strategy for creating this library was sequential cyclic iminium formation and rearrangement under the acidolytic cleavage condition, which yielded unsaturated oxopiperazine structural motifs embedded in various bioactive natural products as dipeptide mimetics. Because of the rigid structure of the unsaturated oxopiperazine, core skeletons with amide or carbamate moiety contained rotational isomers that could not be separated by HPLC; however, we clearly identified each rotamer by conducting an NMR study. The optimized synthetic protocol was tolerant toward various building blocks, and the desired library members were synthesized in parallel with excellent overall yields and purities. The Δ^5-2-oxopiperazine library can be completely realized with extensive diversification at the R_1-R_3 positions; however, we demonstrated the practicality and efficiency of this novel pathway through the construction of a pilot library with 192 members. Biological evaluation of this library is currently in progress. The evaluation results and focused library construction will be reported in the near future.

Experimental Section

General Information. All commercially available reagents and solvents were used without further purification unless noted otherwise. All the solvents, such as DMF, methanol, dichloromethane, and DMSO, were of HPLC degree and purchased from Aldrich and Baker. Bromoacetal resins were obtained from either Advanced ChemTech or Aldrich, but the high-loading resins for actual library construction were synthesized in our laboratory. The reaction steps for the library construction were performed in parallel using the

FlexChem Synthesis System from SciGene (Sunnyvale, CA) in a 96-deep-well filtration block. The reaction volume per well in the 96-well reaction block was set to 1.2 mL unless noted otherwise. The purity of all the library members was observed by HPLC/MS spectra recorded on a Water Alliance LC/MS system, which comprised a Micromass Quattromicro mass spectrometer, photodiode array detector, and 2795 HT-HPLC system equipped with Thermo Hypersil Gold column (C-18, 50 × 2.1 mm, 5 μm). NMR spectra were obtained on Bruker 300 MHz and Varian INOVA 500 MHz spectrophotometers. Chemical shifts (δ_H) are quoted in parts per million (ppm) and referenced to TMS and DMSO-d_6

General Solid-Phase Reaction Procedures. Step 1: Amine Substitution. Bromoacetal resins (40 mg, 1.6 mmol/g, 0.064 mmol) were loaded into each well of a Robbins 96-deep-well filtration block, and solutions of 12 different R_1 -amines (20 equiv in 1.2 mL of DMSO) were dispensed into the designated wells of the reaction block. The reaction mixture was shaken at 60 °C in a rotating oven (Robbins Scientific) for 12 h. The resins thus obtained were washed extensively with DMF, MeOH, and DCM sequentially (three times each) and dried in a high-vacuum desiccator.

Step 2: Amino Acid Coupling. A reaction cocktail of *N*-Fmoc(*O*-*t*-Bu)Tyr-OH (Senn Chem AG, Switzerland) (3 equiv), HATU (3 equiv), and DIPEA (6 equiv) in DMF (1.2 mL per well) was added to each well charged with the resins. After the reaction mixture was incubated in a rotating oven for 12 h at room temperature, the resins were washed extensively with DMF, MeOH, and DCM sequentially (three times each) and dried in a high-vacuum desiccator.

Step 3a: Acid Coupling. Twenty-five percent piperidine in DMF was added to the resins in the reaction block, and the reaction mixture was shaken for 1 h at room temperature to unmask the Fmoc-protected primary amine. The resins were then washed extensively with DMF, methanol, DCM, and DMF, in that order. The activated ester for the acid coupling was generated in situ by the activation of carboxylic acids (3 equiv) with DIC (3 equiv) and HOBt (3 equiv) in DMF for 30 min. The resulting reaction cocktail was dispensed into the designated wells charged with resins, and the reaction mixture was incubated in a rotating oven for 12 h at room temperature. The resins were then washed extensively with DMF, MeOH, and DCM sequentially and dried in a high-vacuum desiccator.

Step 3b: Isocyanate Coupling. Twenty-five percent piperidine in DMF was added to the resin in the reaction block, and the reaction mixture was shaken for 1 h at room temperature. The resins were washed extensively with DMF, MeOH, and DCM sequentially. A reaction cocktail of isocyanate (3 equiv) and DIPEA (3 equiv) in dichloroethane (DCE) was dispensed into the designated wells charged with resins, and the reaction mixture was incubated in a rotating oven for 5 h at room temperature. The resins were washed with DMF, MeOH, and DCM, in that order, and dried in a high-vacuum desiccator.

Step 3c: Chloroformate Coupling. Twenty-five percent piperidine in DMF was added to the resin in the reaction block, and the reaction mixture was shaken for 1 h at room temperature. The resins were washed extensively with DMF, MeOH, and DCM sequentially. A solution of chloroformate (3 equiv) and DIPEA (3 equiv) in DCE was dispensed into the wells charged with resins, and the reaction mixture was incubated in a rotating oven for 5 h at room temperature. The resins were washed with DMF, MeOH, and DCM, in that order, and dried in a high-vacuum desiccator

Step 4: Cleavage and Cyclization. The resins in the reaction block were first dried under high vacuum and then treated with 100% formic acid (1.4 mL per well) for 3 h at 60 °C. After resin removal by filtration, the filtrate was condensed in vacuo using SpeedVac (Thermo Savant) to yield the desired product as a film. The products were diluted with 50% water/acetonitrile and freeze-dried: a process that yielded a pale yellow powder. The purity of the final products was observed by LC/MS without further purification.

Characterization of Compound 5a. The compound exists as a 1:1 mixture of amide rotamers. Signals corresponding to the major rotamer. ^{1}H NMR (300 MHz, $CDCl_3$): δ 7.29 (m, 5H), 6.93 (m, 2H), 6.66 (m, 3H), 5.78 (d, J = 5.8, 1H), 5.43 (t, J = 6.8, 1H), 4.66(m, 2H), 2.86 (m, 2H), 2.01 (s, 3H). Representative signals corresponding to the minor rotamer. ^{1}H NMR (300 MHz, $CDCl_3$): δ 6.68 (m, 1H), 5.93 (d, J = 5.8, 1H), 5.47 (d, J = 5.8, 1H), 4.54 (m, 1H), 1.40 (s, 3H). ^{13}C NMR (125 MHz, $CDCl_3$): δ 19.7, 20.8, 34.5, 35.0, 48.6, 48.8, 56.1, 61.6, 107.5, 108.6, 115.0, 115.7, 127.7, 127.9, 128.7, 130.3, 130.5, 154.9, 165.1. LC/MS (ESI$^+$) Calcd for $C_{20}H_{21}N_2O_3$ $[M + H]^+$: *m*/*z* 337.16. Found: *m*/*z* 337.06.

Characterization of Compound 5b. The compound exists as a 3:2 mixture of amide rotamers. Signals corresponding to the major rotamer. ^{1}H NMR (300 MHz, $CDCl_3$): δ 7.34−7.12 (m, 10H), 6.89 (m, 2H), 6.59 (d, J = 8.3, 2H), 6.35, (d, J = 5.9, 1H), 5.54 (d, J = 5.9, 1H), 5.00 (m, 2H), 4.91-(m, 1H), 4.65 (m, 2H), 2.89 (m, 2H). Representative signals corresponding to the minor rotamer. ^{1}H NMR (300 MHz, $CDCl_3$): δ 6.15 (d, J = 5.9, 1H), 5.32 (d, J = 5.9, 1H), 5.08 (m, 1H). ^{13}C NMR (125 MHz, $CDCl_3$): δ 29.7, 35.4, 48.9, 59.1, 68.1, 108.7, 109.0, 111.8, 112.9, 115.3, 127.5, 128.0, 128.1, 128.3, 128.4, 128.6, 128.8, 130.7, 135.1, 135.7, 135.9, 152.5, 153.2, 154.8, 164.7. LC/MS (ESI$^+$) Calcd for $C_{26}H_{25}N_2O_4$ $[M + H]^+$: *m*/*z* 429.18. Found: *m*/*z* 429.19.

Characterization of Compound 5c. ^{1}H NMR (300 MHz, $CDCl_3$): δ 7.25 (m, 8H), 7.04(m, 2H), 6.93 (d, J = 8.3, 2H), 6.71 (bs, 1H), 6.61 (d, J = 8.3, 2H), 6.21, (d, J = 5.9, 1H), 5.59 (d, J = 5.9, 1H), 4.75 (br, 1H), 4.69 (dd, J = 57.8, 14.7, 2H), 4.39(m, 1H), 4.25 (dd, J = 14.2, 5.8, 1H), 3.99 (dd, J = 14.2, 4.4, 1H), 2.86 (m, 2H). ^{13}C NMR (125 MHz, $CDCl_3$): δ 34.7, 45.1, 48.9, 108.6, 113.0, 115.8, 127.2, 127.5, 127.8, 127.9, 128.5, 128.6, 128.8, 130.4, 135.9, 137.8, 154.5, 155.6, 157.9, 164.4. LC/MS (ESI$^+$) Calcd for $C_{26}H_{26}N_3O_3$ $[M + H]^+$ *m*/*z* 428.20. Found: *m*/*z* 428.12.

Representative Compounds of Library Members in Table 2. Characterization of Compound 9{*1, 3*}. The compound exists as a 3:2 mixture of amide rotamers. Signals corresponding to the major rotamer. ^{1}H NMR (300 MHz, $CDCl_3$): δ 7.23 (m, 4H), 7.02 (m, 1H), 6.87 (d, J = 8.4, 2H), 6.55 (d, J = 8.4, 2H), 5.98 (dd, J = 4.2, 1.8, 1H), 5.49 (d, J = 5.9, 1H), 5.43 (m, 1H), 3.66 (s, 2H), 3.45 − 3.03 (m, 3H), 2.98−2.70 (m, 2H), 2.03−1.61 (m, 1H), 0.84 (m,

6H). Representative signals corresponding to the minor rotamer. ^{1}H NMR (300 MHz, $CDCl_3$): δ 6.96 (m, 2H), 6.72-(m, 1H), 6.67(m, 2H), 5.80 (d, J = 5.9, 1H), 4.61 (m, 1H), 3.79 (s, 2H). LC/MS (ESI^+) Calcd for $C_{23}H_{27}N_2O_3$ $[M + H]^+$: m/z 379.20. Found: m/z 379.15.

Characterization of Compound 9{*3, 3*}. The compound exists as a 2:1 mixture of amide rotamers. Signals corresponding to the major rotamer. ^{1}H NMR (300 MHz, $CDCl_3$): δ 7.25 (m, 8H), 7.02 (m, 1H), 6.89 (m, 1H), 6.85 (d, J = 8.3, 2H), 6.54 (d, J = 8.3, 2H), 5.98 (dd, J = 5.8, 1.5, 1H), 5.44 (d, J = 5.8, 1H), 5.43 (m, 1H), 3.66 (s, 2H), 3.65−3.35 (m, 2H), 3.00−2.55 (m, 2H), 2.61 (m 2H), 1.89 (m, 2H). Representative signals corresponding to the minor rotamer. ^{1}H NMR (300 MHz, $CDCl_3$): δ 6.97 (d, J = 8.4, 2H), 6.72 (dd, J = 4.2, 1.6, 1H), 6.66 (d, J = 8.4, 2H), 5.78 (d, J = 6.0, 1H), 4.62 (m, 1H). LC/MS (ESI^+) Calcd for $C_{28}H_{29}N_2O_3$ $[M + H]^+$: m/z 441.21. Found: 441.16.

Characterization of Compound 9{*5, 9*}. The compound exists as a 7:5 mixture of amide rotamers. Signals corresponding to the major rotamer. ^{1}H NMR (300 MHz, $CDCl_3$): δ 6.99 (m, 2H), 6.68 (m, 2H), 6.35 (t, J = 5.0, 1H), 5.83 (dd, J = 9.9, 4.8, 1H), 4.86 (m, 1H), 4.03 (m, 1H), 3.84 (m, 1H), 3.75 (m, 2H), 3.42 (m, 1H), 3.37 (s, 3H), 2.86 (m, 2H), 1.89 (m, 3H), 1.54 (m, 1H). Representative signals corresponding to the minor rotamer. ^{1}H NMR (300 MHz, $CDCl_3$): δ 6.14 (t, J = 5.0, 1H), 5.65 (dd, J = 26.2, 5.7, 1H), 5.01 (m, 1H), 3.67 (s, 3H). LC/MS (ESI^+) Calcd for $C_{18}H_{23}N_2O_5$ $[M + H]^+$: m/z 347.16. Found: m/z 346.99.

Characterization of Compound 9{*6, 9*}. The compound exists as a 3:2 mixture of amide rotamers. Signals corresponding to the major rotamer. ^{1}H NMR (300 MHz, $CDCl_3$): δ 6.96 (m, 2H), 6.67 (m, 2H), 6.36 (d, J = 6.0, 1H), 5.56 (d, J = 6.0, 1H), 4.82 (m, 1H), 3.45 (m, 2H), 3.39 (s, 3H), 2.83 (m, 2H), 1.57 (m, 1H), 1.42 (m, 2H), 0.91 (d, J = 6.5, 6H). Representative signals corresponding to the minor rotamer. ^{1}H NMR (300 MHz, $CDCl_3$): δ 6.14 (d, J = 5.9, 1H), 5.37 (d, J = 5.9, 1H), 4.98 (t, J = 6.0, 1H), 3.68 (s, 3H). LC/MS (ESI^+) Calcd for $C_{18}H_{25}N_2O_4$ $[M + H]^+$: m/z 333.18. Found: m/z 333.04.

Characterization of Compound 9{*8, 12*}. ^{1}H NMR (300 MHz, $CDCl_3$): δ 7.23 (m, 5H), 7.06 (d, J = 6.9, 2H), 6.93 (d, J = 8.9, 2H), 6.67 (d, J = 8.4, 2H), 6.14 (br, 1H), 5.59 (d, J = 5.7, 1H), 4.54 (bs, 1H), 4.07 (bs, 1H), 3.71−3.42 (m, 2H), 3.39−3.25 (m, 4H), 3.30 (s, 3H), 2.81 (m, 2H), 2.47 (m, 2H), 1.87 (m, 2H). LC/MS (ESI^+) Calcd for $C_{24}H_{30}N_3O_4$ $[M + H]^+$: 424.22. Found: 424.18 $[M + H]^+$.

Characterization of Compound 9{*12, 12*}. ^{1}H NMR (300 MHz, $CDCl_3$): δ 7.42 (bs, 1H), 7.23 (m, 3H), 7.04 (d, J = 6.9, 2H), 6.94 (d, J = 8.3, 2H), 6.67 (d, J = 8.3, 2H), 6.18 (bs, 1H), 5.57 (d, J = 5.75, 1H), 4.49 (bs, 1H), 3.37 (m, 1H), 3.24 (m, 2H), 3.05−2.73 (m, 3H), 2.42 (m, 2H), 1.67 (m, 7H), 1.24 (m, 3H), 0.89 (m, 2H). LC/MS (ESI^+) Calcd for $C_{27}H_{34}N_3O_3$ $[M + H]^+$: m/z 448.26. Found: m/z 448.21.

Acknowledgment. This study was supported by a grant (CBM2-B113-001-1-0-0) from the Center for Biological Modulators of the 21st Century Frontier R&D Program, the Ministry of Science and Technology, Korea (MOST), the Korean Science and Engineering Foundation (KOSEF), and MarineBio21, Ministry of Maritime Affairs and Fisheries, Korea (MOMAF).

Supporting Information Available. ^{1}H NMR, COSY, HPLC, and mass spectra for the representative library members, complete NMR study (COSY and NOESY) to confirm the presence of the rotamers in compound **5a** associated with the data analysis, and LC/MS spectra (PDA detector) of the 192 representative final compounds of this library without further purification. This material is available free of charge via the Internet at http://pubs.acs.org.

References and Notes

(1) Rossen, K.; Sager, J.; DiMichele, L. M. *Tetrahedron Lett.* **1997**, *38*, 3183 and references cited therein.
(2) (a) Guo, C.; Reich, S.; Showalter, R.; Villafranca, E.; Dong, L. *Tetrahedron Lett.* **2000**, *41*, 5307. (b) Matsumoto, E. WO0107419, 2001.
(3) Tong, Y.; Fobian, Y. M.; Wu, M.; Boyd, N. D.; Moeller, K. D. *J. Org. Chem.* **2000**, *65*, 2484.
(4) (a) Askew, B. C., Jr.; Aya, T.; Biswas, K.; Cai, G.; Chen, J. J.; Han, N.; Liu, Q.; Nguyen, T.; Nishimura, N.; Nomak, R.; Peterkin, T.; Qian, W.; Yang, K.; Yuan, C. C.; Zhu, J.; D'amico, D. C.; Nguyen, T.; Qian, W. WO2006019975, 2006. (b) Aya, T.; Cai, G.; Chen, J. J.; D'amico, D. C.; Nguyen, T.; Qian, W. WO2006044355, 2006.
(5) Peng, H.; Carrico, D.; Thai, V.; Blaskovich, M.; Bucher, C.; Pusateri, E. E.; Sebti, S. M.; Hamilton, A. D. *Org. Biomol. Chem.* **2006**, *4*, 1768.
(6) Sugihara, H.; Fukushi, H.; Miyawaki, T.; Imai, Y.; Terashita, Z.; Kawamura, M.; Fujisawa, Y.; Kita, S. *J. Med. Chem.* **1998**, *41*, 489.
(7) Horwell, D. C.; Lewthwaite, R. A.; Pritchard, M. C.; Ratcliffe, G. S.; Rubin, J. R. *Tetrahedron* **1998**, *54*, 4591.
(8) Kitamura, S.; Fukushi, H.; Miyawaki, T.; Kawamura, M.; Konishi, N.; Terashita, Z.; Naka, T. *J. Med. Chem.* **2001**, *44*, 2438.
(9) Clark, E. A.; Golub, T. R.; Lander, E. C.; Hynes, R. O. *Nature* **2000**, *406*, 532.
(10) (a) Okada, Y.; Taguchi, H.; Yokoi, T. *Tetrahedron Lett.* **1996**, *37*, 2249. (b) Su, T.; Yang, H.; Volkots, D.; Woolfrey, J.; Dam, S.; Wong, P.; Sinha, U.; Scarborough, R. M.; Zhu, B. Y. *Bioorg. Med. Chem. Lett*. **2003**, *13*, 729. (c) Sugihara, H.; Terashita, Z.; Fukushi, H. EP 0 643 072 A1, 1995.
(11) Veerman, J. J. N.; Bon, R. S.; Hue, B. T. B.; Girones, D.; Rutjes, F. P. J. T.; Maarseveen, J. H.; Hiemstra, H. *J. Org. Chem.* **2003**, *68*, 4486.
(12) Todd, M. H.; Ndubaku, C.; Bartlett, P. A. *J. Org. Chem.* **2002**, *67*, 3985.
(13) (a) Cheng, J. F.; Chen, M.; Arrhenius, T.; Nadzan, A. *Tetrahedron Lett.* **2002**, *43*, 6293. (b) Cheng, J. F.; Chen, M.; Nadzan, A. M. US 20050113514, 2005.
(14) Miller, J. F.; Spaltenstein, A. *Tetrahedron Lett*. **1996**, *37*, 2521.
(15) Bhatt, U.; Mohamed, N.; Just, G. *Tetrahedron Lett.* **1997**, *38*, 3679.
(16) Ma, H.; Horiuchi, K. Y. *Drug Discovery Today* **2006**, *11*, 661.
(17) Lam, K. S.; Renil, M. *Curr. Opin. Chem. Biol*. **2002**, *6*, 353.
(18) Uttamchandani, M.; Walsh, D. P.; Yao, S. Q.; Chang, Y. T. *Curr. Opin. Chem. Biol*. **2005**, *9*, 4.
(19) (a) Hergenrother, P. J.; Depew, K. M.; Schreiber, S. L. *J. Am. Chem. Soc*. **2000**, *122*, 7849. (b) Barnes-Seeman, D.; Park, S. B.; Koehler, A. N.; Schreiber, S. L. *Angew. Chem., Int. Ed.* **2003**, *42*, 2376. (c) Bradner, J. E.; McPherson, O.

M.; Mazitschek, R.; Barnes-Seeman, D.; Shen, J. P.; Dhaliwal, J.; Stevenson, K. E.; Duffner, J. L.; Park, S. B.; Neuberg, D. S.; Nghiem, P.; Schreiber, S. L.; Koehler, A. N. *Chem. Biol.* **2006**, *13*, 493.

(20) Maryanoff, B. E.; Zhang, H. C.; Cohen, H. H.; Turchi, I. J.; Cynthia, M. A. *Chem. Rev.* **2004**, *104*, 1431.

(21) Kurihara, H.; Mishima, H. *Heterocycles* **1982**, *17*, 191.

(22) (a) Lee, S.-C.; Park, S. B. *J. Comb. Chem.* **2006**, *8*, 50. (b) Lee, S. -C.; Choi, S. Y.; Chung, Y. K.; Park, S. B. *Tetrahedron Lett.* **2006**, *47*, 6843.

CC0700492